Pergamon

Int. J. Solids Structures Vol. 32, No. 23, pp. 3451–3464, 1995

0020–7683/95 $9.50 + .00

0020–7683(94)00317–3

LANDSLIDES MODELED AS BIFURCATIONS OF CREEPING SLOPES WITH NONLINEAR FRICTION LAW

K.T. CHAU
Department of Civil and Structural Engineering, The Hong Kong Polytechnic University, Hung Hom, Hong Kong

(*Received* 4 *September* 1994; *in revised form* 8 *December* 1994)

Abstract—This paper investigates landslide as a consequence of the unstable slide of an initially stationary or creeping slope triggered by a small perturbation, such as the effect due to rainfall. Motivated by Skempton's (1985) observation on clay and siltstone containing low clay fraction, the one state variable friction law proposed by Ruina (1983), in which shear resistance along the slip surface (τ) depends on both sliding history (or the state) and the creeping velocity of the slope (V), is extended to model both fluid-saturated rock and soil joints. Presuming that the slope is shallow and infinitely long, a system of three coupled nonlinear first-order differential equations, relating τ, V and u (displacement of the slip surface), is formulated. Linear stability analysis suggests that an equilibrium state (or a critical point) of a slope can be classified as either an asymptotically stable spiral point, an asymptotically stable improper point, or an asymptotically unstable saddle point in the dimensionless shear stress–velocity (s–v) phase plane, depending on the state parameters on the slip surface. For the special case that steady state τ is insensitive to V and the gravitational pull equals the threshold shear stress (τ_0), the critical point becomes a neutrally stable equilibrium line in the s–v phase plane; trajectories in the s–v phase plane are obtained analytically for this case. Periodic solution (or Hopf bifurcation) for the system is ruled out based on physical grounds. A fully nonlinear numerical analysis is done for all possible scenarios when a finite perturbation is imposed to the equilibrium state. As the slip continues and erosion due to rainfall occurs, nonlinear parameters of the slip surface may evolve such that a previously stable slope may become unstable (i.e. bifurcation occurs) when a small perturbation is imposed. Thus, the present analysis offers a plausible explanation to why slope failure occurs at a particular rainfall, which is not the largest in the history of the slope.

1. INTRODUCTION

Many landslides around the world were triggered by rainfall [e.g. Kim *et al.* (1991); Pierson *et al.* (1991); Polloni *et al.* (1991); Premchitt *et al.* (1994)]. The effect of perched ground water level on slope stability has been studied extensively [e.g. Iverson (1991); Varadarajan *et al.* (1980); Moriwaki (1985); Sammori and Tsuboyama (1991)]. However, there is a concern that statistical relation between rainfall data and landslide occurrence may lead to the pitfalls associated with such predictions (Bhandari *et al.*, 1991).

In particular, there remain many intriguing unanswered questions relating to rainfall triggered landslides. For examples, at a particular hill-side under heavy rainfall, why one slope fails while the adjacent slopes stand, even though the rainfall data and slope type are virtually the same? How can one explain that the failure of a particular slope occurring at a rainfall which is not the largest in the history of the slope? Traditional slope stability analysis based on limit analysis surely cannot answer these questions. In order to capture the subtle nature of slope failure after rainfall, the state and the nonlinear constitutive response of a slip surface must be incorporated in order to achieve a better prediction of landslide.

This paper investigates the possibility that failure of slopes along rock joints or soil interfaces is a consequence of unstable slide bifurcated from a stationary or creeping slope when it is subjected to a small perturbation, such as a sudden change in either the shear stress or velocity along the slip surface after heavy rainfall. Although the stability of creeping slope has been studied by Savage and Chleborad (1982) and Davis *et al.* (1990, 1993), the feature of nonlinear friction law and its consequence on landslide have not been fully explored. Motivated by the laboratory data on dry rock joints (Dieterich, 1979;

Ruina, 1983; Tullis and Weeks, 1986; and others) and on fluid-saturated clay and siltstone containing low clay fraction (Skempton, 1985), we adopt in this study the one state variable friction law proposed by Ruina (1983). Note that for slopes with no well-defined slip surface, such as rock joint or soil interface, an analysis for progressive failure should be incorporated (e.g. Palmer and Rice, 1973); such analysis is, however, out of the scope of the present study.

Although the applicability of the state variable approach to dry rock joints has been studied extensively (Ruina, 1983: Rice and Ruina, 1983: Gu *et al.*, 1984; Tullis and Weeks, 1986: and others), its possible application to water-saturated (wet) slip surface or joints has not been investigated. Motivated by the experimental results for saturated clay by Skempton (1985), we propose here that the dry friction law proposed by Ruina (1983) applies equally to slip surface containing saturated clay. In particular, Skempton (1985) reported that, in the ring shear test for clay, the shear stress along the slip surface jumps to a higher value if a sudden change in the sliding velocity is imposed, and decreases to a new steady state as the sliding continues. This is exactly the same as the jump phenomenon, described by Ruina (1983) and others, observed for dry rock joints driven by a spring attached to the upper rock block.

Note that although most of Skempton's (1985) experimental results were done on clay undergoing "fast rate sliding" (sliding velocity $V > 0.01$ mm min^{-1}), such as those induced by earthquakes, the same phenomenon was also observed on fluid-saturated clay with much slower sliding rate ($V < 0.01$ mm min^{-1}). In particular, the last peak in Fig. 20 and the second to last peak in Fig. 23 of Skempton (1985) show clearly that jumps in shear stress exist before the shear stresses decrease to the steady state value, despite that the magnitude of jumps is much smaller compared with those occurring at "fast rate tests" and that there is no significant change in the residual shear strength. Nevertheless, this lends credence to the universality of the "jump phenomenon" regardless of the displacement rate along the slip surface. Furthermore, Skempton (1985) also suggested that the jumps in shear stresses are induced by the negative pore pressure generated by the sudden increase in sliding velocity. If his conjecture is correct, the jump phenomenon should appear at all sliding rates.

The aim of this paper is to provide a general framework which applies the one state variable friction law to landslide problems. To make the problem mathematically tractable, we only consider here shallow landslides (mostly for natural slopes) which can be idealized by infinite slope assumptions. In particular, driven by the gravitational pull, the sliding soil or rock mass is basically equivalent to a single sliding block with a frictional surface at the bottom. By force equilibrium parallel to the slope surface, a system of three coupled nonlinear first-order differential equations is formulated. Linear stability analysis is then applied to study the possible behavior when small perturbation is imposed to a stationary or creeping slope. However, nonlinear numerically stability analyses will be considered when the system is finitely perturbed, by imposition of a sudden jump in either the friction stress or the creeping velocity. The effect of rainfall enters the analysis only through the sudden change in either shear stress or creeping velocity; i.e., it is considered as a triggering factor of slope instability.

2. NONLINEAR STATE VARIABLE FRICTION LAW

In this section, motivated by Skempton's (1985) data we propose that the one state variable dry friction law by Ruina (1983) applies equally to wet slip surfaces containing saturated clay. Presuming that the memory dependence of the slip surface, either a fluid-saturated soil interface or a fluid-saturated rock joint, can be reasonably represented by a current state variable, which itself evolves with ongoing slip, the constitutive response of the slip surface is characterized by (Ruina, 1983):

$$\tau = \tau_0 + \theta + A \ln (V/V_0), \tag{1}$$

$$\frac{d\theta}{dt} = -\frac{V}{L}[\theta + B \ln (V/V_0)], \tag{2}$$

where V is the slip velocity, V_0 is the reference velocity, A and B are empirical constants, τ_0 is the threshold stress level, t is the time variable, and L is a characteristic decay length scale. For $V \equiv 0$, we normally assume that Coulomb's friction law applies; that is: $\tau_0 = \mu\sigma$, where μ and σ are the frictional coefficient and the normal stress at the slip surface. The state variable θ is introduced to characterize the current mechanical state of the slip surface. The parameters, A, B, L, τ_0 and θ, distinguish one slip surface from the others, even though they may be composed of the same material. In general, θ remains constant for steady state, but evolves for unsteady slip.

Figure 1(a–c) reports some experimental results for friction stress variations with slip rate changes for Quartzite rock joint (Ruina, 1983), Kalabagh Dam clay, and siltstone with

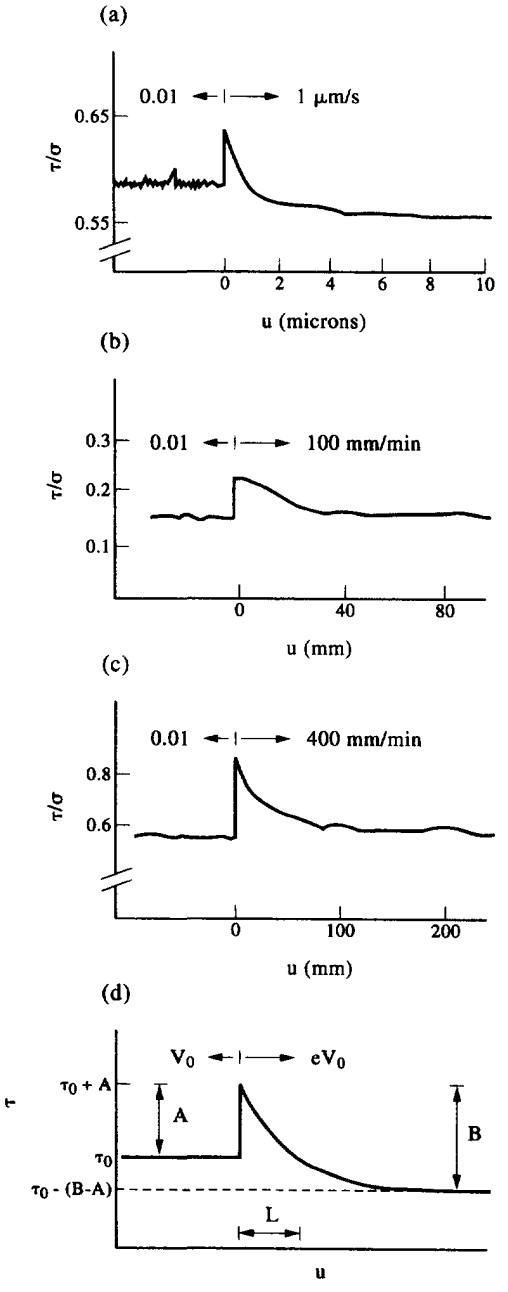

Fig. 1. Frictional stress variation with the change in sliding velocity observed experimentally and predicted by eqns (1) and (2). Experimental plots are: (a) Quartzite rock joint (after Ruina, 1983), (b) Kalabagh Dam clay (after Skempton, 1985), and (c) siltstone with low clay fraction (after Skempton, 1985); and theoretical prediction is given in (d) by the one state variable friction law.

low clay fraction (Skempton, 1985) respectively; and a typical prediction by eqns (1) and (2) is given in Fig. 1(d). In particular, eqns (1) and (2) predict that the shear stress along the slip surface increases by A when the velocity increases suddenly from V_0 to eV_0 ($e \sim 2.71828$), and then decreases exponentially with ongoing slip by amount B, with a characteristic decay length of L. As θ evolves with ongoing slip, a new steady state value $-B\ln(V/V_0)$ will be approached; and the new steady state stress becomes:

$$\tau_{ss} = \tau_0 + (A-B)\ln(V/V_0). \tag{3}$$

Differentiating eqn (3) with respect to V, we have the velocity dependency of τ:

$$\frac{d\tau_{ss}}{dV} = \frac{1}{V}(A-B). \tag{4}$$

The slip surface is velocity strengthening if $A-B>0$ (i.e. $d\tau_{ss}/dV>0$), and is velocity softening if $A-B<0$ (i.e. $d\tau_{ss}/dV<0$). As shown by Ruina (1983), such a response of eqns (1) and (2) is capable of describing the laboratory observations. We refer to Ruina (1983), Rice and Ruina (1983), Gu *et al.* (1984), Tullis and Weeks (1986) and other for more detailed description of this one state variable constitutive framework.

Figure 1(b,c) shows typical results of rate dependency on saturated clay obtained by the ring shear test (Skempton, 1985). Note that the shear stress suffers a jump as the slip rate is increased suddenly, and follows by an exponentially decay with the ongoing slip. This suggests that eqns (1) and (2) apply equally well in describing the wet (fluid-saturated) friction phenomenon although this framework was originally motivated by a dry friction experiment on rock surface. Although Fig 1(b,c) is extracted from the results of fast-rate tests ($V>0.01$ mm min^{-1}), a similar phenomenon, as discussed in the Introduction, is expected for much slower creeping rates, which are more likely to be observed in creeping slopes.

Based upon the above nonlinear constitutive description of the slip surface, a system of equations for infinite creeping slopes is formulated next.

3. FORMULATION FOR CREEPING SLOPES

To investigate the effect of nonlinear state variable friction law in a reasonably simple way, we consider in this paper the stability problem of a long slope with a pre-existing slip surface, probably a soil interface filled with softer clay or a rock joint filled with gouge. A slope at equilibrium is either initially stationary or creeping steadily at a very slow rate. When a perturbation in either shear stress or velocity is imposed, the force equilibrium will simply be the balance of the gravitational pull, the self weight of the overlying rock or soil mass, and the inertia force along the direction parallel to the slope surface. As shown in Fig. 2, it is mathematically equivalent to replacing the translational sliding slope by a single sliding block. Consequently, the acceleration of the sliding mass is:

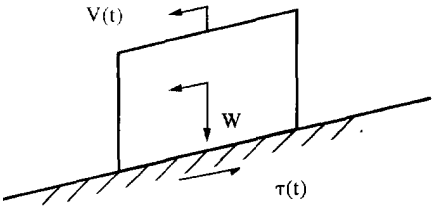

Fig. 2. The force equilibrium for an idealized infinite slope with sliding velocity $V(t)$ and overlying weight W, and subject to a shear stress $\tau(t)$ at the bottom.

$$\frac{dV}{dt} = g\sin i - \frac{\tau}{\rho h}, \tag{5}$$

where g is the gravitational constant (≈ 9.81 m s^{-2}), i the slope angle, ρ the mass density, and h the thickness of the overlying soil or rock mass. Differentiating eqn (1) with respect to time, we obtain:

$$\frac{d\tau}{dt} = \frac{d\theta}{dt} + \frac{A}{V}\frac{dV}{dt}. \tag{6}$$

Substitution of eqns (2) and (5) into eqn (6) leads to:

$$\frac{d\tau}{dt} = -\frac{V}{L}[\theta + B\ln(V/V_0)] + \frac{A}{\rho h V}(\rho g h\sin i - \tau). \tag{7}$$

Equations (7), (2), (5) and the displacement–velocity relation (i.e. $du/dt = V$, where u is the sliding displacement) form a system of four first-order differential equations for τ, V, θ and u. However, θ can be eliminated by using eqn (1); and the system of equations is reduced to:

$$\frac{d\tau}{dt} = -\frac{V}{L}[\tau - \tau_0 + (B-A)\ln(V/V_0)] + \frac{A}{\rho h V}(\rho g h\sin i - \tau), \tag{8}$$

$$\frac{dV}{dt} = \frac{1}{\rho h}(\rho g h\sin i - \tau), \tag{9}$$

$$\frac{du}{dt} = V. \tag{10}$$

The solution of eqns (8)–(10) gives $\tau(t)$, $V(t)$ and $u(t)$; then $\theta(t)$ can be found by using eqn (1). Before we proceed to consider the possible behavior of this nonlinear system, it is convenient to introduce the following dimensionless stress (s), velocity (v), displacement (δ), and time (T):

$$s = \tau/A, \quad v = \ln(V/V_0), \quad \delta = u/h, \quad T = V_0 t/h. \tag{11}$$

The nonlinear system can then be rewritten as:

$$\frac{ds}{dT} = -\lambda e^{v}[s - s_0 - (1-\beta)v] + \frac{e^{-v}}{\kappa}(\gamma - s), \tag{12}$$

$$\frac{dv}{dT} = \frac{e^{-v}}{\kappa}(\gamma - s), \tag{13}$$

$$\frac{d\delta}{dT} = e^{v}, \tag{14}$$

where $s_0 = \tau_0/A$, $\kappa = \rho V_0^2/A$, $\gamma = \rho g h\sin i/A$, $\beta = B/A$, and $\lambda = h/L$. Note that the system is *autonomous*, since the rates of s, v and δ do not contain time variable (T) explicitly. Because the system (12)–(14) is nonlinear, exact solutions for s, v and δ are, in general, not possible. Thus, it is informative to first consider the possible equilibrium solutions and their corresponding stabilities, before we try to solve the system numerically.

4. LINEAR STABILITY ANALYSIS OF THE SYSTEM

The equilibrium or so-called critical point of the system can be obtained by setting: $ds/dT = dv/dT = 0$ [e.g. Minorsky (1962); Boyce and DiPrima (1986)]. The critical point in the s–v phase plane is:

$$s = \bar{s} = \gamma, \quad v = \bar{v} = \frac{\gamma - s_0}{1-\beta}. \tag{15}$$

This corresponds to the rate of changes of s and v to vanish simultaneously. Thus, a steady sliding slope is always possible if force equilibrium is satisfied. A stationary slope is a special case of this critical point when the gravitational pull equals the threshold shear stress; i.e. $s_0 = \gamma$ and $\bar{v} = 0$. Note that the solutions $s(T)$ and $v(T)$ will form trajectories on the s–v phase plane.

It is important to know whether a stationary or steadily sliding slope is stable subject to a small perturbation, such as a sudden change in both s and v resulting from a heavy rainfall. Will the steadily sliding slope become unstable ($v \to \infty$ as $T \to \infty$) or remain stable ($v \to \bar{v}$ as $T \to \infty$)?

To shed light on this question, we use the phase plane analysis [e.g. Minorsky (1962); Boyce and DiPrima (1986)] for some qualitative information about the equilibrium solution. First, we introduce the new variables:

$$\phi = s - \bar{s}, \quad \psi = v - \bar{v}, \tag{16}$$

which corresponds to the perturbation about the equilibrium point or the critical point $(\bar{s},\bar{v})$; and the critical point becomes the origin in the $\phi-\psi$ space. Substitution of eqn (16) into eqns (12) and (13), the following governing equations for ϕ and ψ are obtained:

$$\frac{d\phi}{dT} = -\left(\lambda e^{\beta} + \frac{e^{-\ell}}{\kappa}\right)\phi + \lambda e^{\beta}(1-\beta)\psi + g_1(\phi,\psi), \tag{17}$$

$$\frac{d\psi}{dT} = -\frac{e^{-\ell}}{\kappa}\phi + g_2(\phi,\psi), \tag{18}$$

where $g_1(\phi,\psi)$ and $g_2(\phi,\psi)$ are the nonlinear terms of the expansion about $(\bar{s},\bar{v})$. It can be shown that both $g_1(\phi,\psi)$ and $g_2(\phi,\psi)$ decay much faster than the distance from the critical point in the sense that:

$$g_1(\phi,\psi)/r \to 0, \quad g_2(\phi,\psi)/r \to 0, \quad \text{as } r \to 0, \tag{19}$$

where $r = (\phi^2+\psi^2)^{1/2}$ is the distance from the origin. Consequently, eqns (17) and (18) are *almost linear* near the critical point. Then, a linear stability analysis can be applied to study the stability near the critical point. In particular, we linearize eqns (17) and (18) by dropping g_1 and g_2, and seek solutions of the form:

$$\phi = c_1 e^{\omega T}, \quad \psi = c_2 e^{\omega T}, \tag{20}$$

where c_1 and c_2 are arbitrary constants. It is straightforward to see that ω is the eigenvalue of the linearized system, and equals:

$$\omega_{1,2} = [p \pm (p^2-4q)^{1/2}]/2, \quad p = -\left(\lambda e^{\beta} + \frac{e^{-\ell}}{\kappa}\right), \quad q = \frac{\lambda}{\kappa}(1-\beta). \tag{21}$$

Note that the radicand in the first part of eqn (21) can be rearranged as:

$$p^2-4q=\left(\lambda e^{\bar{s}}-\frac{e^{-\bar{v}}}{\kappa}\right)^2+\frac{4\lambda\beta}{\kappa}. \tag{22}$$

If λ, β and κ are all positive, the eigenvalue will not be complex (or the critical point will not be a spiral point). Physically λ and κ must be positive, but β may be negative although the results of experiments on rock joint (Ruina, 1983) and clay (Skempton, 1985) strongly suggest that β is positive. In the subsequent discussion, we will not restrict our consideration to positive β.

Note also that $p<0$ for positive λ and κ. Thus, the possibility of periodic solution (or Hopf bifurcation) for s and v is ruled out, since periodic solution corresponds to $p=0$ and $q>0$ (i.e. ω_1 and ω_2 are purely imaginary). For $p<0$, the critical point (or the steady state solution) will not be an unstable spiral point (i.e. ω_1 and ω_2 are a complex conjugate pair with positive real part) or unstable improper node (i.e. ω_1 and ω_2 are real positive numbers of unequal magnitude). Consequently, the critical point can only be either an asymptotically stable spiral point, an asymptotically improper node, or an unstable saddle point (Section 5 will show further that the critical point can also be "a neutrally stable equilibrium line" for the special case that $\beta=1$ and $\gamma=s_0$). These possible scenarios are summarized in Fig. 3; and their corresponding stabilities are summarized here:

4.1. *Spiral points with asymptotic stability*

If the parameters of the slip surface satisfy: $p<0$; $p^2-4q<0$, the eigenvalues become a complex conjugate pair with a negative real part. As remarked earlier, $p<0$ is always satisfied, and $p^2-4q<0$ yields:

$$\beta<-\frac{\kappa}{4\lambda}\left(\lambda e^{\bar{s}}-\frac{e^{-\bar{v}}}{\kappa}\right)^2. \tag{23}$$

Thus, if β is negative and satisfied eqn (23), the critical point is an asymptotically stable spiral point. This implies that B must be negative for positive A. Although both the experimental results by Ruina (1983) and Skempton (1985) suggest that A and B are of the same sign, we do not rule out such possibility here. In particular, a *small* perturbation about the steady state solution $(\bar{s},\bar{v})$ will result in a solution $[s(T),v(T)]$ forming a trajectory moving spirally towards the equilibrium point $(\bar{s},\bar{v})$ as shown in Fig. 3. Theoretically, the solution approaches the critical point as origin as $T\to\infty$. When the slope is subjected to a

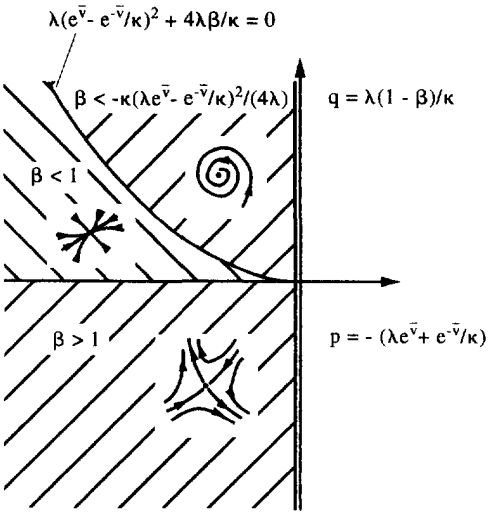

Fig. 3. Regime classification for three possible types of equilibrium point in the p–q parameter space. In particular, $\beta<-\kappa(\lambda e^{\bar{s}}-e^{-\bar{v}}/\kappa)^2/(4\lambda)$ for asymptotically stable spiral points, $\beta<1$ for asymptotically stable improper nodes, and $\beta<1$ for unstable saddle points.

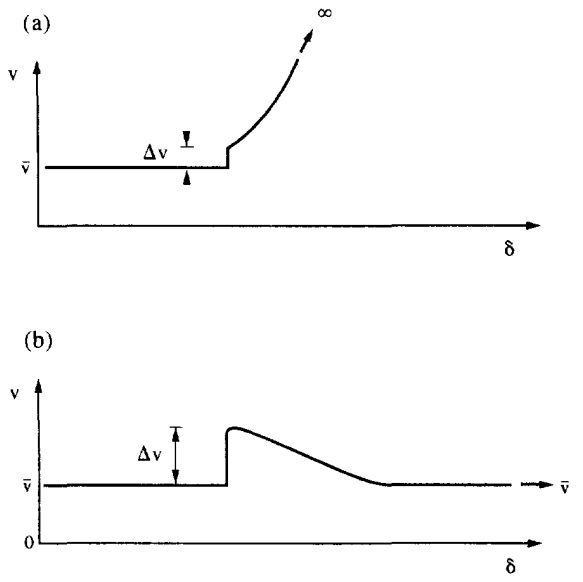

Fig. 4. Sketches for velocity evolutions when the sliding velocity is suddenly increased to $\bar{v}+\Delta v$: (a) for unstable response; (b) for stable response.

small change in v, a typical velocity response with displacement is shown in Fig. 4(b). That is, the solution is asymptotically stable in the sense that if ϕ and ψ are *small*, and the trajectories of the linear system are satisfactory approximations to those of the *actual* nonlinear system eqns (17) and (18). But, what is *small*? Or, what is the region of asymptotic stability, beyond which $g_1(\phi, \psi)$ and $g_2(\phi, \psi)$ are no longer negligible? We must go back to the original nonlinear system and study numerically the set of initial conditions for which a critical point is asymptotically stable; as will be shown in Section 5 that the linear analysis approximates the actual response adequately even for finite perturbation in s or v.

4.2. *Improper nodes with asymptotic stability*

If the parameters of the slip surface satisfy: $q > 0$; $p^2 - 4q \geqslant 0$, the eigenvalues are real negative and unequal ($\omega_1 < \omega_2 < 0$). This implies that $\beta < 1$, or $A > B$. Note that the condition of velocity strengthening [see eqn (4)] merges with the condition for the critical point being an improper node with asymptotic stability. In particular, any *small* perturbation about the critical point will result in a solution approaching the origin, and it also tends toward the direction of the eigenvector corresponding to ω_2. Again, when the system is subjected to a small change in v, a typical velocity evolution with displacement is given in Fig. 4(b). However, if the initial perturbed point is exactly on a line of the direction of the eigenvector corresponding to ω_1, the solution will remain on the direction and approach the origin as $t \to \infty$. Again the region of asymptotic stability should be estimated numerically if the perturbation is not small; the numerical results will be given in Section 5.

4.3. *Unstable saddle points*

For this case, the eigenvalues are real and of opposite sign (i.e. $\omega_1 > 0 > \omega_2$), and the parameters satisfy: $q < 0$ and $p^2 - 4q > 0$. These conditions are satisfied if $\beta > 1$ or $B > A$. The experimental results of Ruina (1983) for dry rock joints give $B > A$; and, Skempton's (1985) results on clay joints give $A < B$. That is, $B > A$ is always a possibility, depending on the state and mechanical properties of the slip surface. If the initial perturbed state is on the line along the direction of the eigenvector corresponding to ω_2, the solution will remain on the line and approach the critical point at the origin as $T \to \infty$, because the solution contains only a negative exponential term. For all other initial states, the positive exponential term will dominate for large T, so eventually all solutions approach infinity asymptotic to the line determined by the eigenvector corresponding to ω_1, as shown in Fig. 3.

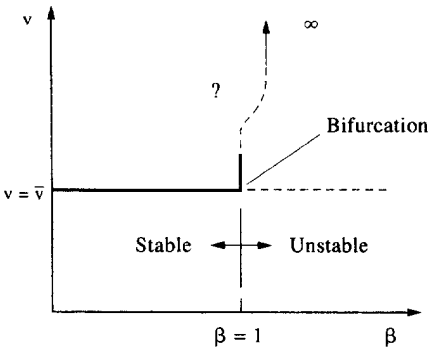

Fig. 5. The β-dependency of the velocity measure v. The equilibrium state $v = \bar{v}$ is stable for $\beta < 1$ (indicated by a solid line) and unstable for $\beta > 1$ (indicated by a dashed line). The bifurcation point is at $\beta = 1$: the dashed segment of the curve with appended question mark is intended to indicate qualitatively a larger value of v.

This is the most crucial case among all three possible scenarios. Physically, if a small perturbation is imposed to an equilibrium state (a saddle point), such as the effect of earthquake or rainfall on the slip surface, a stationary or steady creeping slope will become unstable. Eventually as $v(T)$ increases drastically, catastrophic landslides will result (see Fig. 4(a) for a sketch of the response). Note that, in general, rainfall will increase the pore pressure at the slip surface; consequently, it decreases s and increases v. Thus, the effect of rainfall is equivalent to adding a negative Δs and a positive Δv as perturbation. So far, we have assumed that the system is autonomous (or physically the parameters of the system are time-dependent). However, if β of a slip surface is < 1 (i.e. the equilibrium state is an asymptotically unstable improper node) and is allowed to change, probably due to erosion by previous heavy rainfall, it may happen that $\beta > 1$ is resulted after a series of heavy rainfall (i.e. the stable improper node evolves to an unstable saddle point). Then, if a slope containing such a slip surface is perturbed by a rainfall (which may be much smaller than the previous ones), it will cause a catastrophic landslide. Mathematically, β can be considered as a nonlinear parameter; $\beta = 1$ corresponds to a bifurcation point, at which unstable slide bifurcates from the primary state $v = \bar{v}$. The situation can be summarized with reference to Fig. 5, which shows the β-dependency of the velocity v. The dashed curve segment of the bifurcation with an appended question mark is intended for only qualitative indication of large v.

The argument given here suggests that slope failure may be triggered by a rainfall which is not the largest in the history of the slope, depending on the evolution of the parameters of the slope caused by its environment. Thus, the present analysis provides a new feature which is more attractive than the conventional slope stability analysis.

Note also that the condition for a critical point being an unstable saddle point merges with the condition for velocity softening.

5. NONLINEAR STABILITY ANALYSIS OF THE SYSTEM

The previous section is based on a linear stability analysis near the critical point. Now we return to the nonlinear system (12)–(14). The solutions of this autonomous system can be described as curves, or often called trajectories, on the s–v phase plane. Instead of solving the system (12)–(14), these trajectories can be found by solving a related first-order differential equation:

$$\frac{ds}{dv} = 1 - \frac{\lambda\kappa}{(\gamma - s)}[s - s_0 - v(1-\beta)]e^{2v}, \tag{24}$$

which is obtained by combining eqns (12) and (13). Alternatively, this can be written in differential form as:

$$(\gamma - s)\,\mathrm{d}s + \{\lambda\kappa[s - s_0 - v(1-\beta)]\mathrm{e}^{2v} - \gamma + s\}\,\mathrm{d}v = 0. \tag{25}$$

The left side is not a perfect differential but we can multiply eqn (25) by an integrating factor $\mathrm{e}^{f}(s, v)$ to get

$$\mathrm{d}P(s, v) = \mathrm{e}^{f(s,v)}(\gamma - s)\,\mathrm{d}s + \mathrm{e}^{f(s,v)}\{\lambda\kappa[s - s_0 - v(1-\beta)]\mathrm{e}^{2v} - \gamma + s\}\,\mathrm{d}v = 0. \tag{26}$$

That is, we seek a function $P(s, v) = C$ (where C is a constant), which is a trajectory of the solution in the s–v phase plane. Denoting P_v and P_s as the coefficients of $\mathrm{d}v$ and $\mathrm{d}s$ in eqn (26) respectively, the condition for an exact differential requires that $\partial P_v/\partial s = \partial P_s/\partial v$, which then yields

$$(\gamma - s)\frac{\partial f}{\partial v} - \{\lambda\kappa[s - s_0 - v(1-\beta)]\mathrm{e}^{2v} - \gamma + s\}\frac{\partial f}{\partial s} - (\lambda\kappa\mathrm{e}^{2v} + 1) = 0. \tag{27}$$

Once $f(s, v)$ in eqn (27) is solved, the function $P(s, v) = C$ can be found. Consequently, the trajectories of the solution in the phase plane for the nonlinear system (12)–(14) can be used to study the stability of the system. However, the integrating factor $f(s, v)$ can only be found in special cases.

5.1. *Trajectories for neutrally stable equilibrium lines*

In particular, if $\beta = 1$ and $\gamma = s_0$, a solution for eqn (27) is $f = -\ln(s - s_0)$. Then, the trajectories can be obtained by integrating eqn (26) as:

$$P = -s + \frac{\lambda\kappa}{2}\mathrm{e}^{2v} + v = C, \tag{28}$$

where C is a constant. Although the trajectories can be solved analytically only for this particular case, the state of $\beta = 1$ and $\gamma = s_0$ corresponds to an interesting situation. As we remarked previously, the critical point changes from an asymptotically stable improper node to an unstable saddle point when $\beta < 1$ changes to $\beta > 1$. Thus, $\beta = 1$ is a transition point between two different types of stability. Physically, as demonstrated in Fig. 1, it corresponds to $A = B$, or to the case that the steady state shear stress τ_{ss} is insensitive to the sliding velocity V. Skempton's (1985) results suggest that such situation is quite possible for clay and siltstone with low clay fraction, in which the steady state residual strength is roughly the same for different V. The condition $\gamma = s_0$ implies the gravitational pull along the slip plane due to overlying soil or rock mass equal to the threshold shear stress level; i.e. the slip surface is an quasi-static equilibrium. Note that the $\beta = 1$ the critical point becomes the line $s = s_0$ with v arbitrary, i.e. when the forces are in equilibrium and the friction law is rate-insensitive, any initial constant slip velocity can be an equilibrium state.

Figure 6 shows typical trajectories for various $P = C$ given in eqn (28); the dashed horizontal line is the equilibrium line $s = s_0$. The plot is for $\lambda = 1.5$, $\kappa = 2.0$ and $\gamma = \beta = s_0 = 1.0$. Note that for the larger v (say $v \geqslant 2$), the exponential term in eqn (28) will dominate and trajectories become essentially independent of s, as shown in Fig. 6. The directions of the arrows shown in Fig. 6 seem to suggest that the equilibrium line is stable. More precisely, as shown in Fig. 7, the equilibrium should be classified as *neutrally stable* in the sense that a finite perturbation about a equilibrium state $s = s_0$ and $v = v_0$ will result in solutions forming trajectories being attracted back to either the original state (point O) or a neighbouring state (point E or F), depending on the perturbation. In particular, if a perturbation $(\Delta s, \Delta v)$ is applied along either OA or OB, which satisfies: $P = P_0$ (where $P_0 = -s_0 + \lambda\kappa\exp(2v_0)/2 + v_0$), equilibrium point is stable. However, when the stress s is suddenly increased by Δs_1 along OC, the new resulting equilibrium state will be at E, as sliding evolves along CE according to $P = P_1 (P_1 = P_0 - \Delta s_1)$. The new sliding velocity v_1 will be smaller than v_0 as $P_1 < P_0$. Conversely, if a sudden drop in s by $-\Delta s_2$ is imposed along OD, a new equilibrium state F will be resulted along DF which satisfies

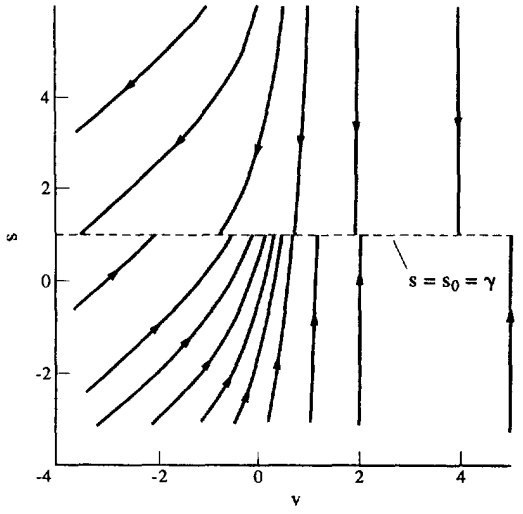

Fig. 6. Trajectories of the solutions around a neutrally stable equilibrium line $s = s_0$ in s–v phase plane. The plot is for $\lambda = 1.5$, $\kappa = 2.0$, and $\gamma = \beta = s_0 = 1.0$.

$P = P_2 = P_0 + \Delta s_1$. In short, a small perturbation to the system will result in a new equilibrium state which can be arbitrarily close to the original state, depending on the magnitude of the perturbation. Thus, the system is called neutrally stable, similar to the horizontal rolling of a ball on a frictional surface caused by an applied force.

5.2. *Trajectories for spiral points*

The linear analysis for the trajectories in Section 4 is valid only in the vicinity of the critical points. When the system is finitely perturbed, the trajectories for the nonlinear system can, however, be obtained by solving eqns (12)–(14) or eqn (24) numerically by the fourth-order Runge–Kutta method with error control [e.g. Press *et al.* (1989)]. Figure 8 plots some typical trajectories around a spiral point; the parameters used for the slip surface are: $\beta = -0.5$, $\gamma = 2.5$, $s_0 = 1.0$, $\lambda = 1.5$ and $\kappa = 1.0$. Note that eqn (23) is satisfied; the critical point is at $v = 1.0$ and $s = 2.5$, which is an attractor in the phase plane. The solutions on the phase plane move towards to equilibrium point even though the perturbations in both velocity and stress are finite. Thus, the linear analysis given in Section 4 does provide an accurate prediction of the stability. Note also that, due to the nonlinear terms, the

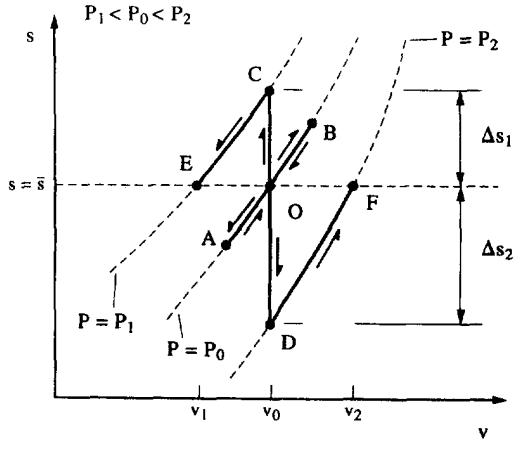

Fig. 7. Responses of a equilibrium line subject to perturbations along OA, OB, OC and OD. The new sliding velocities at E and F are v_1 ($< v_0$) and v_2 ($> v_0$), respectively. The trajectories along AB, CE and DF satisfy the special cases of eqn (28): $P = P_0$, $P = P_1$ ($P_1 = P_0 - \Delta s_1 < P_0$), and $P = P_2$ ($P_2 = P_0 + \Delta s_2 > P_0$), respectively.

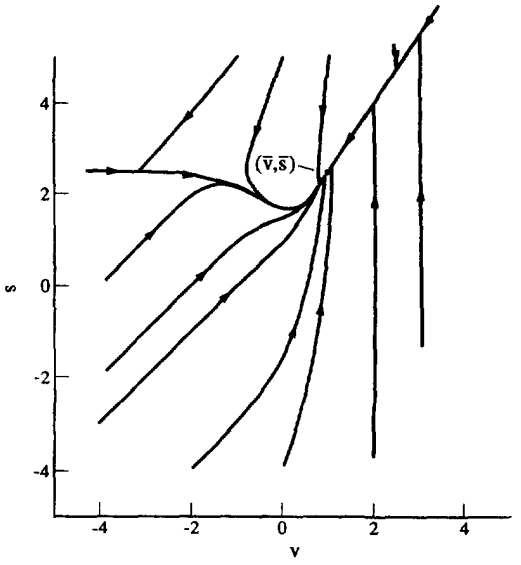

Fig. 8. Typical trajectories for the solutions around a spiral point in the s–v phase plane. The spiral point is at $v = 1.0$ and $s = 2.5$. Trajectories are for $\beta = -0.5$, $\gamma = 2.5$, $s_0 = 1.0$, $\lambda = 1.5$ and $\kappa = 1.0$.

trajectories are not perfectly spiral as suggested by linear stability analysis (Compare Fig. 8 with the sketch on Fig. 3).

5.3. *Trajectories for improper nodes*

Typical trajectories of the solutions near an improper node are given in Fig. 9. the parameters used are: $\beta = 0.5$, $\gamma = 2.0$, $s_0 = 1.0$, $\lambda = 1.5$ and $\kappa = 1.0$. The equilibrium point is at $v = 2.0$ and $s = 2.0$. As shown in the figure, all solutions approach the equilibrium point as $T \to \infty$ along a line with direction parallel to the eigenvector corresponding to the larger eigenvalue. Again, the nonlinear analysis shows that linear analysis given in Section 4 provides an adequate description of the stability of the critical point even when finite perturbation is imposed.

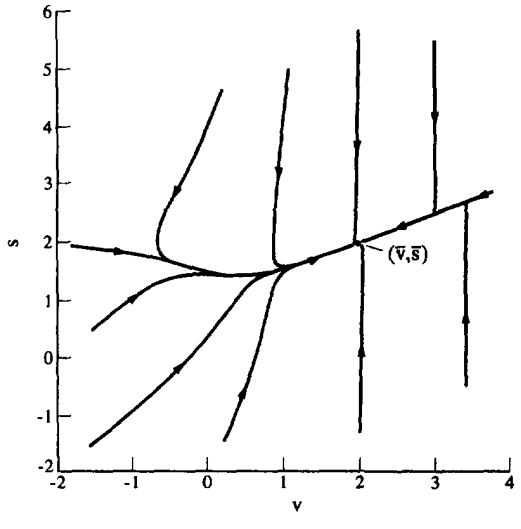

Fig. 9. Typical trajectories for the solutions round an improper node in the s–v phase plane. The improper node is at $v = 2.0$ and $s = 2.0$. Trajectories are for $\beta = 0.5$, $\gamma = 2$, $s_0 = 1.0$, $\lambda = 1.5$ and $\kappa = 1.0$.

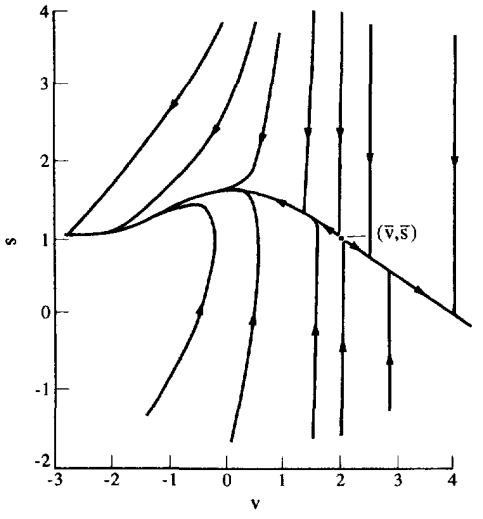

Fig. 10. Typical trajectories for the solutions round a saddle point in the s–v phase plane. The saddle point is at $v = 2.0$ and $s = 1.0$. Trajectories are for $\beta = 1.5$, $\gamma = 1.0$, $s_0 = 2.0$, $\lambda = 1.5$ and $\kappa = 1.0$.

5.4. *Trajectories for saddle points*

Typical trajectories around a saddle point are depicted in Fig. 10. The parameters used in the plot are: $\beta = 1.5$, $\gamma = 1.0$, $s_0 = 2.0$, $\lambda = 1.5$ and $\kappa = 1.0$; the corresponding equilibrium point is at $v = 2.0$ and $s = 1.0$. The numerical simulation shows that all solutions of the perturbed system move away from the equilibrium point; i.e. the equilibrium point is unstable. Theoretically, if the perturbation is on the line along the eigenvector of the small eigenvalue, the solution approaches the critical points as $T \to \infty$. However, this stable solution is nearly impossible to be obtained numerically, as a slight deviation off the line will produce an unstable solution.

6. CONCLUSION

In this paper, we have outlined a framework to model landslide as a consequence of unstable creep when the slope is subjected to an external excitation, such as rainfall. Motivated by Skempton's (1985) data for clay and siltstone containing low clay fraction, the one state variable friction law proposed by Ruina (1983) is adopted in this study for soil or rock joints containing saturated clay. To capture the essence of the nonlinear friction law, only infinite slope model is considered. By applying linear analysis, we show that the equilibrium state, either a stationary or steadily creeping slope, is stable if it corresponds to either a stable spiral point or a stable improper node in the s–v phase plane; and it is unstable if the equilibrium state corresponds to an unstable saddle point in the phase plane. For the special case that $\beta = 1$ and $\gamma = s_0$, the equilibrium state becomes a neutrally stable line in the s–v phase plane; the trajectories in the phase plane for this case can be obtained analytically by eqn (28). The validity of the linear analysis is then checked by solving the nonlinear system numerically; typical trajectories around a stable spiral point, a stable improper node, a neutrally stable equilibrium line and an unstable saddle point are given. In addition, it is argued that as slip proceeds and erosion occurs, β (a nonlinear parameter in the system) may increase from $\beta < 1$ to $\beta > 1$. Thus, a stable improper node may evolve to an unstable saddle point, as a result of environmental impact on the slope. Consequently, the present analysis is capable to explain why landslide occurs at a particular rainfall, which is not the largest in the history of the slope [e.g. Chau (1994); Chau and Chan (1994)]. Although the present analysis provides an alternative to the traditional methods, more detailed experimental and theoretical studies are still required.

Acknowledgements—Although this work was originally inspired by a term project and lectures of the "Mechanics of Earthquake" offered by Prof. John Rudnicki, most of it was finished when I was visiting the Rock Mechanics

Research Centre of CSIRO (Commonwealth Scientific and Industrial Research Organization), Perth, Australia in the summer of 1994. I am grateful to the financial support by the Hong Kong Polytechnic University and the CSIRO; and the work cannot be finished without the continuous encouragement and support from my beloved wife, Lim.

REFERENCES

Bhandari, R. K., Senanayake, K. S. and Thayalan, N. (1991). Pitfalls in the prediction on landslide through rainfall data. In *Landslides* (Edited by Bell), pp. 887–890. Balkema, Rotterdam.

Boyce, W. E. and DiPrima, R. C. (1986). *Elementary Differential Equations and Boundary Value Problems* (4th ed). John Wiley, New York.

Chau, K. T. (1994). Failure of slopes modelled as bifurcation. In *Int. Conf. Comp. Meth. Struct. Geot. Engng* 12–14 December, Hong Kong, Vol. 2, pp. 500–505.

Chau, K. T. and Chan, C. H. (1994). Effect of pore pressure on slope failure modelled as bifurcation. In *International Conference on Landslides, Slope Stability and the Safety of Infra-structures*. 13-14 September 1994, Kuala Lumpur, Malaysia pp. 97–104.

Davis, R. O., Desai, C. S. and Smith, N. R. (1993). Stability of motion of translational landslides. *J. Geot. Eng. ASCE* **119,** 420–432.

Davis, R. O., Smith, N. R. and Salt, G. (1990). Pore fluid frictional heating and stability of creeping landslides. *Int. J. Num. Anal. Meth. Geomech.* **14,** 427–443.

Dieterich, J. H. (1979). Modeling of rock friction—1. Experimental results and constitutive equations. *J. Geophys. Res.* **84,** 2161–2168.

Gu, J.-C., Rice, J. R., Ruina, A. L. and Tse, S. T. (1984). Slip motion and stability of a single degree of freedom elastic system with rate and state dependent friction. *J. Mech. Phys. Solids* **32,** 167–196.

Iverson, R. M. (1991). Sensitivity of stability analyses to groundwater data. In *Landslides* (Edited by Bell), pp. 451–457 Balkema, Rotterdam.

Kim, S. K., Hong, W. P. and Kim, Y. M. (1991). Prediction of rainfall-triggered landslides in Korea. In *Landslides* (Edited by Bell), pp. 989–994. Balkema, Rotterdam.

Minorsky, N. (1962). *Nonlinear Oscillations*. Van Nostrand, Princeton.

Moriwaki, H. (1985). Compressive displacement of slope due to rainfall induced subsurface flow. In *Proc. IVth Int. Conf. Field Workshop on Landslides*, Tokyo, pp. 233–238.

Palmer, A. C. and Rice, J. R. (1973). The growth of slip surfaces in the progressive failure of over-consolidated clay. *Proc. R. Soc. Lond. A.* **332,** 527–548.

Pierson, T. C., Iverson, R. M. and Ellen, S. D. (1991). Spatial and temporal distribution of shallow landsliding during intense rainfall, southeastern Oahu, Hawaii. In *Landslides* (Edited by Bell), pp. 1393–1398. Balkema, Rotterdam.

Polloni, G., Ceriani, M., Lauzi, S., Padovan, N. and Crosta, G. (1991). Rainfall and soil slipping events in Valtellina. In *Landslides* (Edited by Bell), pp. 183–188. Balkema, Rotterdam.

Premchitt, J., Brand, E. W. and Chen, P. Y. M. (1994). Rain-induced landslides in Hong Kong, 1972–1992. *Asia Engineer* June, 43–51.

Press, W. H., Flannery, B. P., Teukolsky, S. A. and Vetterling, W. T. (1989). *Numerical Recipes: The Art of Scientific Computing*. Cambridge University Press, Cambridge.

Rice, J. R. and Ruina, A. L. (1983). Stability of steady frictional slipping. *J. Appl. Mech.* **50,** 343–349.

Ruina, A. (1983). Slip instability and state variable friction laws. *J. Geophys. Res.* **88,** 10,359–10,370.

Sammori, T. and Tsuboyama, Y. (1991). Parametric study on slope stability with numerical simulation in consideration of seepage process. In *Landslides* (Edited by Bell), pp. 539–544. Balkema, Rotterdam.

Savage, W. Z. and Chleborad, A. F. (1982). A model for creeping flow in landslides. *Bull. Assoc. Engng Geol.* **19,** 333–338.

Skempton, A. W. (1985). Residual strength of clays in landslides, folded strata and the laboratory. *Geotechnique* **35,** 3–18.

Tullis, T. E. and Weeks, J. D. (1986). Constitutive behaviour and stability of frictional sliding of granite. *Pure Appl. Geophys.* **124,** 383–414.

Varadarajan, A., Kuberan, R. and Tyagi, A. C. (1980). Effect of water flow and earthquake on the stability of natural slopes. In *International Symposium on Landslides*, **Vol. 1,** pp. 303–307.